American Genetic Association

Journal of Heredity, 2018, 29–37
doi:10.1093/jhered/esx100
Symposium Article
Advance Access publication 9 November 2017

OXFORD

Symposium Article

Habitat Heterogeneity, Host Population Structure, and Parasite Local Adaptation

Curtis M. Lively

From the Department of Biology, Indiana University, 1001 East Third Street, Bloomington, IN 47405.

Address correspondence to C. M. Lively at the address above, or e-mail: clively@indiana.edu.

Received April 17, 2017; First decision May 21, 2017; Accepted November 7, 2017.

Corresponding Editor: Christopher Smith

Abstract

Reciprocal-transplant experiments have proven to be a powerful tool for detecting local adaptation (LA). More recently, reciprocal cross-inoculation experiments have been used to evaluate adaptation by parasites to their local host populations. These experiments are conceptually similar to reciprocal-transplant experiments, except that the "environment" (the host population) may have evolved in response to changes in the parasite population. Here, I use analytical tools and computer simulations to determine when parasites would be expected to be more infective to their local host populations than to allopatric host populations. The models assume that parasites have to genetically "match" their hosts in order to infect. I also assumed that different host clones were favored in different populations. When parasite virulence was low, clonal selection outweighed parasite-mediated selection, leading to low host diversity within populations and strong LA by parasites. At intermediate levels of virulence, parasite-mediated selection maintained high levels of host diversity within populations, which reduced or eliminated parasite LA. The loss of parasite LA was not associated with increased infectivity by parasites on allopatric hosts. Instead, the loss of LA was due to a reduction in infectivity of parasites on sympatric hosts. Finally, at high levels of parasite virulence, parasite-mediated selection led to oscillatory host dynamics and weak local adaption by parasites. Across all levels of virulence, the strength of parasite LA closely tracked the degree of host population structure (G_{ST}).

Subject areas: Population structure and phylogeography; Conservation genetics and biodiversity
Keywords: coevolution, local adaptation, population structure, Red Queen dynamics

Adaptive divergence among isolated natural populations is an important component of ecological models of speciation (Richmond and Reeder 2002; Langerhans et al. 2007) and it can provide insights into the process of evolution by natural selection (Schluter 1996). One of the most powerful ways to study adaptive divergence among populations is through reciprocal-transplant experiments. In these experiments, organisms from multiple populations in divergent habitats are transplanted into other habitats, as well as back into their home habitat (e.g., Turesson 1922; Clausen et al. 1940; Clausen et al. 1948; Bradshaw 1960; Williams 1966). When the organisms generally perform better in their home habitat than in allopatric habitats, they are referred to as being locally adapted. Local adaptation (LA) has been revealed in a large number of studies in which organisms have been reciprocally transplanted among divergent habitats (reviews in Kawecki and Ebert 2004; Blanquart et al. 2013; Savolainen et al. 2013; Lascoux et al. 2016).

More recently, conceptually similar experiments, called "reciprocal cross-inoculation experiments," have been conducted in host–parasite systems. Here, hosts from multiple populations are exposed to infectious propagules from sympatric and allopatric parasite populations, usually in "common gardens." The goal has been to determine whether parasites are most infective to their local hosts,

or if hosts are most resistant to their local parasites (e.g., Parker 1985; Lively 1989; Ebert 1994; Koskella 2014; Morran et al. 2014). Although parasites are commonly found to be locally adapted, the results are somewhat mixed (Kaltz and Shykoff 1998; Greischar and Koskella 2007; Hoeksema and Forde 2008). This mixture of results presents an interesting conundrum.

One obvious difference between reciprocal-transplant experiments and reciprocal cross-inoculation experiments involving hosts and parasites is that the host (the "habitat") can evolve in response to the evolution in sympatric parasite populations. This leads naturally to host–parasite coevolution. When should this kind of coevolution lead to LA?

There is now a considerable theoretical literature on LA in coevolving host–parasite interactions. Much of the work has been appropriately focused on the interaction between the strength of parasite-mediated selection and gene flow among populations. Strong selection can generate asynchronous oscillatory dynamics across populations, which can lead to parasite LA, provided gene flow is not too high (Frank 1991; Ladle et al. 1993; Judson 1995; Gandon et al. 1996; Morand et al. 1996; Lively 1999; Gandon 2002; Sasaki et al. 2002; Gandon and Otto 2007). On the other hand, small amounts of parasite gene flow allow for the introduction of genetic diversity, which can increase the rate of evolution in parasite populations, thus fueling the oscillations (Hamilton 1993; Judson 1995). Analytical models have shown further that LA can depend on the relative amounts of gene flow for hosts and parasites, where parasite LA is more likely if selection on parasites is stronger than selection on hosts, and if parasites migrate more than hosts (Gandon 2002; Gandon and Michalakis 2002; Morgan et al. 2005). In addition, spatial structure in the host can be generated by genetic drift in small populations, which can lead to local adaption by parasites (Gandon 2002; Gandon and Nuismer 2009). Finally, spatial structure and LA can result from geographic variation in the strength of selection of parasites on hosts, and vice versa (Nuismer 2006; Gandon and Nuismer 2009). Taken together, the results suggest that LA by parasites to hosts depends on a complex interplay between different factors; but, in general, some degree of population genetic structure is required in the host.

In the present study, I studied adaptation by parasites to local host populations, where the host populations were evolving in different abiotic environments. Host evolution in these different environments led to host population structure in the absence of parasites. The results suggest that, compared to avirulent parasites, moderately virulent parasites can homogenize host populations, thereby reducing host population structure and reducing the degree of local adaption to near zero. This reduction in LA, however, was not caused by an increase in infectivity of parasites on allopatric hosts.

Models

Local Adaptation

Assuming a large host population, and that infection requires that parasites match their host's genotype, the average number of secondary infections across all parasite strains is:

$$\overline{R}_0 = B\sum_{i=1}^{P} p_i h_i, \tag{1}$$

where p_i and h_i are the frequencies of the ith parasite and host genotypes, respectively; and B gives the number of eggs produced by each parasite strain that make contact with a host, whether or not the parasite matches and infects the host. Here, the summation term gives the mean probability of success per propagule taken over all parasites genotypes, and is equal to

$$\sum_{i=1}^{P} p_i h_i = P\mathrm{cov}\left(p_i, h_i\right) + \frac{1}{H} \tag{2}$$

where P is the number of parasite strains, and H is the number of host strains (derivation in Lively 2016). This result depends on the assumption that each parasite strain can only infect one host strain, which is the working assumption of the matching alleles model of infection genetics (Frank 1993, 1994; Otto and Michalakis 1998; Agrawal and Lively 2002), but it seems to be reasonably robust as long as parasites show specificity for infection (Engelstädter and Bonhoeffer 2009; Engelstädter 2015). Critically, $\mathrm{cov}(p_i, h_i)$ gives the within-population covariance between the frequencies of the different parasite genotypes and the frequencies of their matching host genotypes. The $1/H$ term in Equation 2 gives the probability of a successful match in the absence of coevolution, and it provides a baseline for parasite fitness whenever the $\mathrm{cov}(p_i, h_i)$ is equal to zero.

For parasites exposed to an allopatric population of hosts, the average probability of infection is

$$\sum_{i=1}^{P} p_i h_i' = P\mathrm{cov}\left(p_i, h_i'\right) + \frac{1}{H'} \tag{3}$$

where the prime symbol indicates hosts in allopatry. The difference between Equations 2 and 3 conforms to the "home vs. away" definition of Kawecki and Ebert (2004). Similarly, for hosts that are exposed to an allopatric population of parasites, the average probability of infection is:

$$\sum_{i=1}^{P'} p_i' h_i = P'\mathrm{cov}\left(p_i', h_i\right) + \frac{1}{H}. \tag{4}$$

Here, the difference between Equations 2 and 4 conforms to the "local vs. foreign" definition of Kawecki and Ebert (2004). Assuming that migration among populations is not sufficiently strong to overcome local selection, then the average covariances involving allopatric combinations of hosts and parasites should be zero under either definition. Assuming further that the numbers of host and parasite strains are equal in all populations, the difference between the mean probability of success per propagule between sympatric and allopatric exposures could be taken as an estimate of LA, L:

$$L = P \times \mathrm{E}\left[\mathrm{cov}\left(p_i, h_i\right)\right] \tag{5}$$

where the expectation term gives the average within-population covariance over all populations in the metapopulation. Equation 5 is true under either definition of LA for the host–parasite situation considered here. Previous work has shown that the 2 definitions give the same result for LA, in general, although they can be associated with different variances about the mean (Morgan et al. 2005; Blanquart et al. 2013). It is worth emphasizing that Equation 5 assumes that migration among populations is not strong enough to produce spatial correlations in allele frequencies among populations, which reduces population structure (Gandon et al. 1996; Gandon 2002; Gandon and Nuismer 2009).

It is worth noting that the derivation of LA derived here is mathematically different from that derived by Gandon and Nuismer (Nuismer and Gandon 2008; Gandon and Nuismer 2009). Both formulations rely on covariances to determine the degree of LA

by parasites; but in the present study the covariance is focused on the average covariance between matching host–parasite genotypes within populations. It is basically a measure of the average fitness of parasites when exposed to sympatric hosts, minus the average fitness of parasites when exposed to allopatric hosts. In contrast, the formulation by Gandon and Nuismer relies on the spatial covariance of matching host–parasite genotypes across populations. If the covariance term is positive, then parasites are locally adapted; if the covariance term is equal to or less than zero, then parasites are not locally adapted (reviewed in Nuismer 2017). It seems likely that the 2 formulations are simply different ways of saying the same thing, but this has not been shown.

Simulations

The simulation initiated 20 different haploid host populations, each with 9 different clonal host genotypes, which were encoded by 3 alleles at 2 loci (following Lively 2010). The clones were randomly assigned to different initial frequencies in all 20 populations. Fecundity was separately and randomly assigned to the each of the 9 host genotypes within all 20 populations. Hence, different clones would, by chance, have fitness advantages in different populations, but there was no intrinsic advantage averaged over the entire metapopulation. This was meant to mirror the realistic possibility that different host genotypes are most fecund in ecologically different populations; it also leads to a natural way to generate host population structure, which is required for LA by parasites. To implement the fecundity assignments, I randomly assigned host genotypes with a mean fecundity of 10 and a normally distributed standard deviation of either 0.1 or 1.0, where higher standard deviations reflect higher fecundity differences among host genotypes within populations.

Host birth rates were density-dependent, following Maynard Smith and Slatkin (1973). Specifically, the birth rate for uninfected hosts was equal to $b_u/(1 + a_u N)$, where b_u is the maximum number of offspring produced, a_u reflects the sensitivity to competition, and N gives the total number of hosts in a population. The carrying capacity, K under this form of density-depended fecundity is, $K = (b_u - 1)/a_u$. As indicated above, I set the mean maximum offspring number to 10 ($b_u = 10$). I set a_u to 0.0001, thus the average carrying capacity, K, was equal to 90 000 individuals in uninfected populations. Given the large populations size, I assumed that drift was negligible.

The hosts were assumed to be annuals. Each of the populations was initiated at carrying capacity, with randomly chosen frequencies for each genotype. A single infected individual for all 9 host genotypes was then added to all 20 populations. In all subsequent generations, the hosts were infected as juveniles after contacting the infectious propagules left from hosts in the previous generation. The parasites were assumed to be asexual. The number of infected hosts for each clone depended on the number of hosts from the same clone that were infected in the previous generation. Specifically, the number of infected juveniles for each host genotype was calculated as,

$$I_{i(t+1)} = h_{i(t+1)} N_{(t+1)} \left[1 - \exp\left(-BI_{i(t)} / N_{(t+1)}\right)\right],$$

where I_i is the number of infected individuals for the ith host type. The expression in brackets gives the probability of infection, assuming that exposure to a single matching parasite genotype is sufficient to cause infection. Thus, the probability of infection increases with the number of infected hosts in the previous generation, which allows for epidemiological feedbacks that can increase the strength of parasite-mediated selection (Lively 2010). Similarly, the number of uninfected juvenile hosts for each genotype was calculated as

$$U_{i(t+1)} = h_{i(t+1)} N_{(t+1)} \left[\exp\left(-BI_{i(t)} / N_{(t+1)}\right)\right].$$

Here, the expression in brackets gives the Poisson distributed probability that the host is not exposed to one or more infectious propagules that match its genotype.

Parasite virulence was assumed to be density-independent ($a_u = a_i$). To vary virulence, I simply reduced the maximum birth rate for infected individuals, b_i, in discrete steps: 9.9, 9, 8, 7, 6, 5, 4, 3, 2, 1, 0.1. Virulence was then calculated as $(b_u - b_i)/b_u$, and thus ranged from 0.01 to 0.99.

I also allowed realized parasite fecundity, B, to vary among populations to capture the biologically realistic idea that ecological differences among populations would affect the probability that parasite propagules make contact with hosts. Hence realized parasite fecundity was initiated separately in each population with a mean of 15, and with a normally distributed variance of 15. I set the variance equal to the mean to model the situation where realized parasite fecundity is random across populations. This approach differs from Nuismer's (2006) approach, which allowed virulence to vary among populations; but it should have a similar effect in creating a geographic mosaic in which the strength of parasite-mediated selection varies among sites.

To simulate host and parasite migration, I coded the simulation to introduce a single infected individual for each host clone with a probability of 0.5. Hence, a single infected migrant for each clone was introduced, on average, every other generation. The total number of infected migrants was then, on average, 4.5 individuals per generation. Because the host populations were large even when infected (>45 000 individuals), the overall host migration rate was small ($m < 0.0001$). The parasite populations were smaller than the host populations, so the migration rate was proportionately higher in the parasite population, but still less than 0.001. Note that there was no bias in the probability of migration by the different infected host genotypes, as they were expected to be equally frequent across the metapopulation. Migrants were assumed to be drawn from a very large metapopulation, of which the 20 simulated populations were only a small part. This is a nonstandard way to simulate "migration," but the main purpose was to introduced genetic variation into the parasite population, which can be lost when virulence is very high (e.g., Lively 1999). Setting migration to zero yielded the same results for virulence levels of 0.8 or less.

The simulation was run for 2100 generations; the data from each of the 20 populations was collected at the final generation. This was meant to capture the system at a single time point in the way in which field biologists might sample a metapopulations. In the absence of parasites, the most fecund clones would become fixed, or nearly fixed, and the host populations became highly structured. Data collected at generation 1000 were similar to those collected at generation 2100, so I assumed that the dynamics had stabilized in 2100 generations.

At generation 2100, I calculated the mean probability of infection across all sympatric combinations of host and parasite ($N = 20$) using Equation 2. I also calculated the mean probability of infection for 20 allopatric combinations of host and parasites, using a different allopatric host for each of the 20 different parasite population (Equation 3), and a different allopatric parasite for each host population (Equation 4). I also calculated the average of the within-population genetic variation for host populations, $H_S = E[1 - \sum \bar{b}_i^2]$, as well as the total genetic variation across the 20 metapopulations, $H_T = 1 - \sum \bar{b}_i^2$, , and the population genetic structure, $G_{ST} = (H_T - H_S)/H_T$ (Nei 1973, 1977; Hedrick 2000). Both measures have

a theoretical maximum when the variance in host genotype frequencies is equal to 0, giving $1 - H(1/H)^2$, which for the present study ($H = 9$) is approximately equal to 0.89. Finally, to measure the degree of oscillation in host genotype frequencies over time, I calculated the average standard deviation in frequency separately for each host genotype for the last 100 generations of the simulation. I then averaged these values to produce a single measure of oscillatory behavior in each host population.

The results reported here show the output for a single run of the simulation for each combination of parameter values. To determine the robustness of the results, I re-ran the simulation 4 additional times to examine the variation among runs for the results reported in Figure 1a. To further determine the robustness of the results, I ran simulations with different combinations of migration by infected and uninfected hosts. In these simulations, the probability of a single infected host entering a population was either 0.1 or 1.0, and the probability of a single uninfected host was either 0.1 or 1.0 (giving 4 different combinations of migration probabilities). I also ran simulations in which I reduced the among-population variance in parasite fecundity for 15 to 0.01, which reduces strength of parasite-mediated selection among populations. Finally, I ran simulations in which 2 different recombination rates were considered (0.05 and 0.50) in a sexual host population. Thus, there was either very low recombination between the 2 host immune loci (0.05), or free recombination between loci (0.50). For these simulations, I used 0.01 (instead of 0.1 or 1.0) for the variance in host fecundity, as recombination would allow selection on host fecundity to be decoupled from selection for parasite resistance.

Results

Given Equation 3, we would expect that parasite populations given to allopatric host populations would have an average probability of infection of $1/H$, which is equal to 0.11 (as H, the number of host genotypes was set at 9 for all 20 host populations). This expectation was met for all values of virulence (e.g., Figure 1a,b). Hence, as expected under the condition of low migration, the covariance term in Equation 3 was very near zero for allopatric exposures. The same results were obtained for the average infection probabilities, whether parasites were exposed to allopatric hosts (Equation 3), or hosts were exposed to allopatric parasites (Equation 4) (Supplementary Figure S1), so only the former (home vs. away) is shown in the main text. The variances about the mean also did not differ between the 2 definitions (Supplementary Figure S1). This later result (equal variances) might be expected, as the simulated exposures mimicked a common garden experiment under ideal conditions for exposure (Blanquart et al. 2013). Finally, the covariance between matching host and parasite genotypes very closely tracked the variance in frequency for the host genotypes (Supplementary Figure S1)

For sympatric combinations of parasite and host, parasite virulence had a decisively nonmonotonic effect on the probability infection (Figure 1a), as well as on the strength of LA (Figure 1e). At low levels of parasite virulence, and when the variance in host fecundity was high, sympatric parasite populations showed high levels of infection (Figure 1a) and strong LA (Figure 1e). The strength of parasite LA decreased when virulence was increased to intermediate levels, and then increased again as virulence was increased to high levels (Figure 1a). Hence, the magnitude of LA showed an asymmetric U-shaped pattern. These results were shown to be qualitatively robust for all 4 independent runs across all virulence values (Supplementary Figure S2).

Total host genetic diversity across the metapopulation (H_T) was only slightly affected by virulence, and remained near its theoretical maximum of 0.89, which implies that the host genotype frequencies were nearly even across the metapopulation (Figure 1c). The average genetic variation within host populations (H_S), however, showed a hump-shaped pattern, with low values of H_S at both low virulence and high virulence, and with high values (near the theoretical max.) of H_S at intermediate levels of virulence (Figure 1c). Thus, H_S was inversely related to the probability of infection in sympatric combinations (compare Figure 1a with Figure 1c). In addition, the measure of population structure, G_{ST}, mapped onto LA in an almost one-to-one manner (Figure 1e). G_{ST} and LA were both high at low levels of parasite virulence, where fecundity selection in the host was strong relative to infection-mediated selection, leading to the loss of host diversity within populations (Figure 1e). G_{ST} and LA were both low at intermediate levels of virulence, when parasite mediated-selection was strong enough to reduce the variation in the frequency of host genotypes. Finally, at high levels of parasite virulence, the populations began to show oscillatory dynamics, which is now known as Red Queen dynamics (Figure 1c). The oscillations reduced the within population genetic variation for populations sampled at a single point in time, thus reducing H_S and increasing G_{ST}.

To test this explanation, I reduced the variance in host fecundity from 1.0 to 0.1. As expected, the observed levels of G_{ST} and LA were much lower at low levels of parasite virulence, as parasite-mediated selection became stronger than fecundity selection, leading to higher levels of within-population variation for hosts (Figure 1b,d,f). Thus negative-frequency dependent selection that is strong relative to host fecundity selection can lead to the homogenization of host populations and the loss to local parasite adaptation. It is worth noting, however, that the loss of parasite LA is not due to the parasites becoming better able to infect allopatric hosts (Figure 1a,b). The probability of infection for allopatric combinations remained low at $1/H$ across all levels of virulence.

These results were robust to changes in the relative migration rates of infected and uninfected hosts (Figure 2). Nonetheless, the number of migrants was very low when compared to population size. The results were also robust to changing the among-population variance in parasite fecundity, B (Figure 3). Reducing the variance in B from 15 to 0.01 had only minor effects on the observed patterns (compare Figure 1a,b to Figure 3a,b). Taken together, the main patterns in the results were qualitatively robust across all combinations of migration rates. They were also robust to within-population fecundity variation among host clones, and to variation in parasite fecundity among parasite populations.

Finally, I relaxed the assumption of clonal host reproduction by introducing recombination between the 2 disease resistance loci. I also assumed that, in a sexual host population, within-habitat selection on fecundity would be decoupled from selection on resistance. As expected, the parasites population showed no sign of LA at low levels of virulence. However, for high levels of virulence, frequency-dependent selection caused cycling in host and parasite genotype frequencies, along some degree of host population structure and LA by parasites (Figure 4). The degree of LA observed, however, was small relative to that observed in clonal host populations (compare Figure 4 to Figure 1).

Discussion

I studied a computer simulation of host–parasite interactions in host populations facing 2 sources of natural selection. One source of

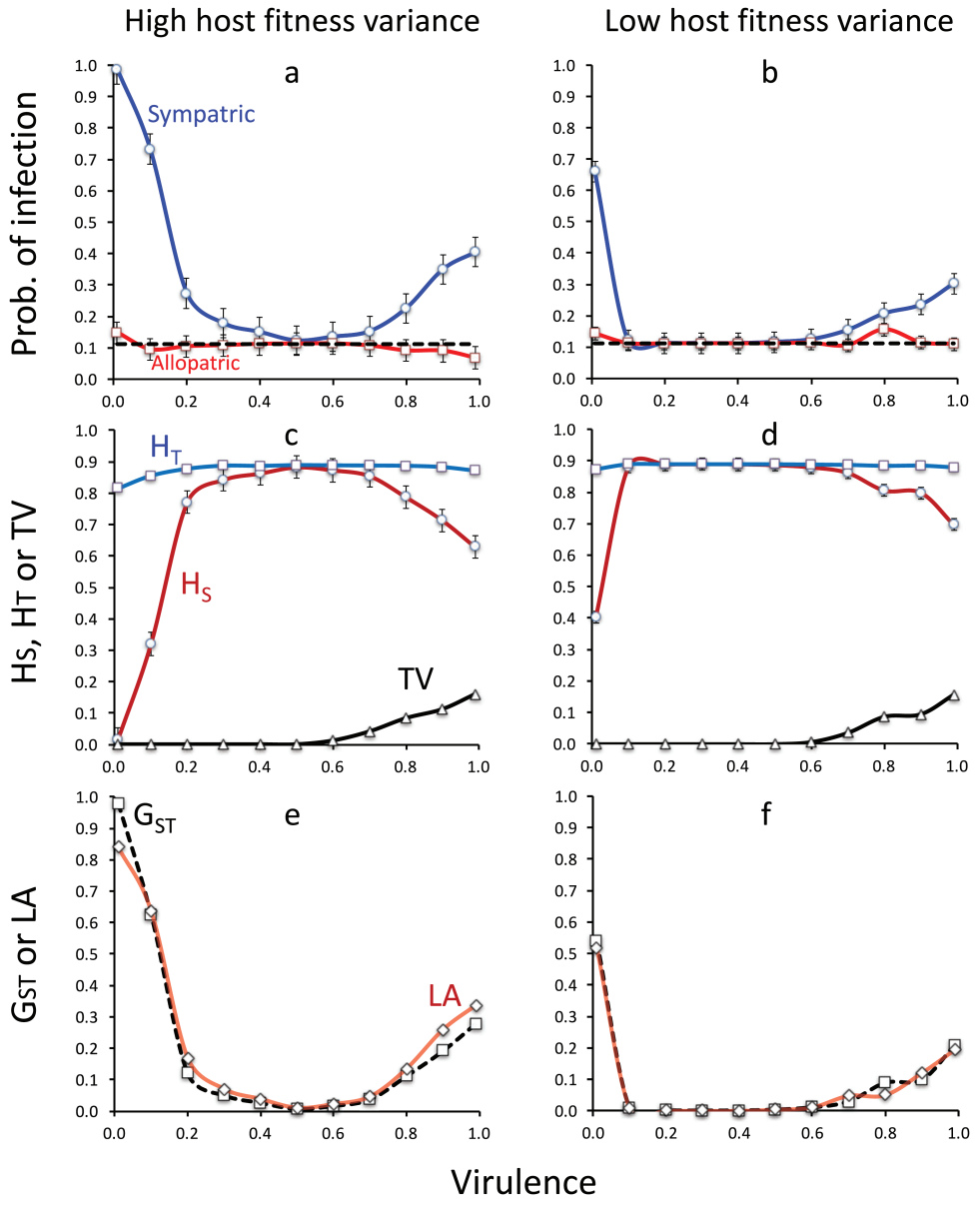

Figure 1. Results from computer simulations. The left-hand column gives the results for relatively high fecundity variance in the host population (standard deviation [STD] = 1); the right-hand column shows results for relatively low variance in host fecundity (STD = 0.1). The top row (**a** and **b**) gives the average probability of infection per parasite propagule for hosts exposed to sympatric parasites (Equation 2, blue line with circles) and for hosts exposed to allopatric parasites (Equation 3, red line with squares). The dashed line in **a** and **b** gives the analytical prediction for infection when the covariance term in Equation 2 or 3 is equal to zero. The middle row (**c** and **d**) gives the mean genetic variation within host populations (*HS,* blue line with squares), the total variation across all 20 populations (*HT,* red line with circles), and the average temporal variation (TV) in genotype frequencies (solid black line). Note that *HT* is near the theoretical maximum of 0.89 over most of the parameter space; and that *HS* is near the theoretical maximum for intermediate values of parasite virulence. The theoretical maximum implies that the variance in host genotype frequencies is very near zero. The bottom row (**e** and **f**) gives LA (red line with diamonds) as the difference between the mean of the sympatric and allopatric populations in panels **a** and **b**, respectively; it also shows the measure of population genetic structure, G_{ST} (dashed black line). In all panels, the probability that a single infected host migrated into a population was 0.5 for all host genotypes. Parasite fecundity (*B*) was set at 15 with a variance of 15 to give variation among populations in the strength of parasite-mediated selection. Error bars give the 95% confidence interval of the mean (calculated as the average across all levels of virulence).

selection was abiotic and frequency-independent; it stemmed from fecundity differences among different host genotypes in different isolated demes. The other source of selection was parasite-mediated, frequency-dependent selection against common host genotypes. The simulations assumed that migration was weak relative to selection, and that a genetic match of hosts by parasites was required for infection. The goal was to determine when parasites might be expected to be locally adapted across a wide range of values for parasite virulence. The simulations assumed a best-case scenario for local parasite adaptation (matching alleles for infection, clonal host reproduction, and low migration), yet parasite LA was not ubiquitous. Relaxing these assumptions would likely further reduce the parameter space under which local parasite adaptation might be expected.

When parasite virulence was relatively low, fecundity selection eroded the within-deme genetic variance in the host population, leading to high values of GST. Parasites then evolved to infect the

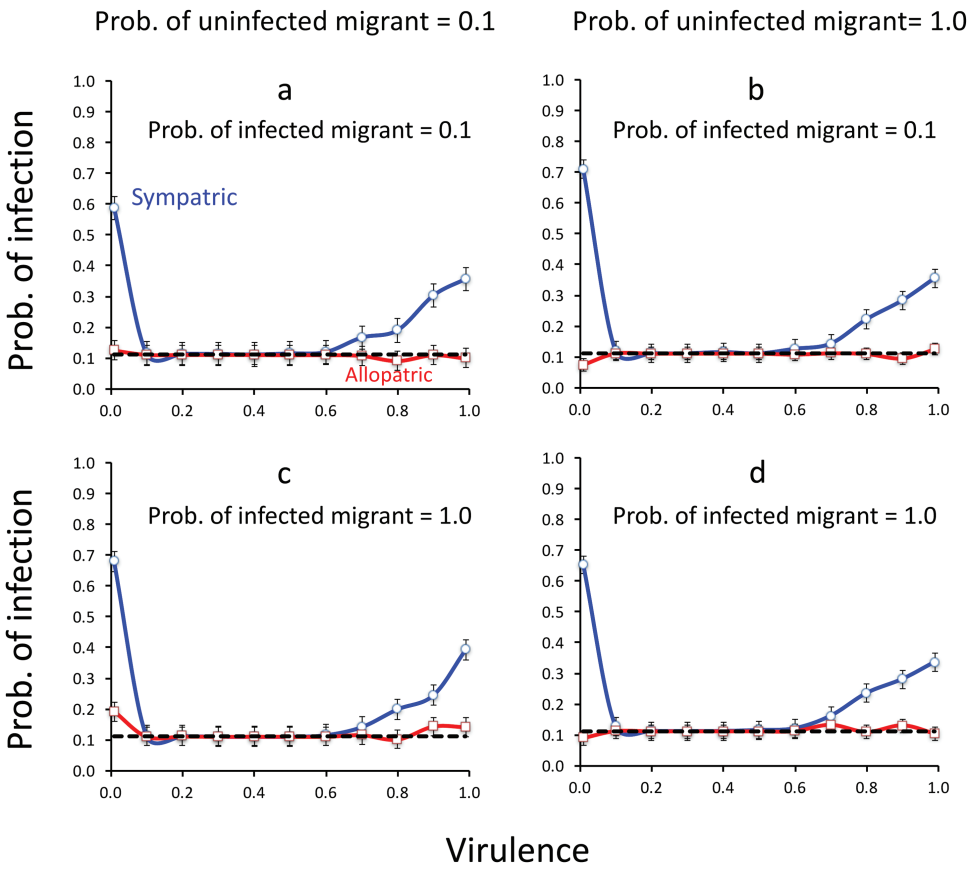

Figure 2. Migration by infected and uninfected hosts. The top row (**a** and **b**) gives the results for simulations where the probability of that a single, infected migrant entered the populations was equal to 0.1 for all host genotypes. The bottom row (**c** and **d**) gives the results for simulations where the probability that a single, infected migrant entered the populations was equal to 1.0 for all host genotypes. Panels on the left (**a** and **c**) give the results for simulations where the probability that a single uninfected host migrant entered the population was 0.1, whereas the right column gives the results where this same probability was 1.0 for all host genotypes. The blue lines (with circles) show the average probability of infection for sympatric parasites, and the red line (with squares) gives the average probability of infection for allopatric parasites. The difference between the 2 lines gives the degree of local parasite adaptation. The dashed line gives the analytical prediction for infection when the covariance term in Equation 2 or 3 is equal to zero. Note that, as expected under low levels of migration, allopatric exposures gave values that are very close to the dashed line for all levels of virulence. Sympatric exposures converge on the dashed line for intermediate levels of virulence. In all panels, the standard deviation in host fecundity within populations was 0.1 (as in the right-hand column in Figure 1). Error bars give the 95% confidence interval of the mean (calculated as the average of the 95% CIs across all levels of parasite virulence).

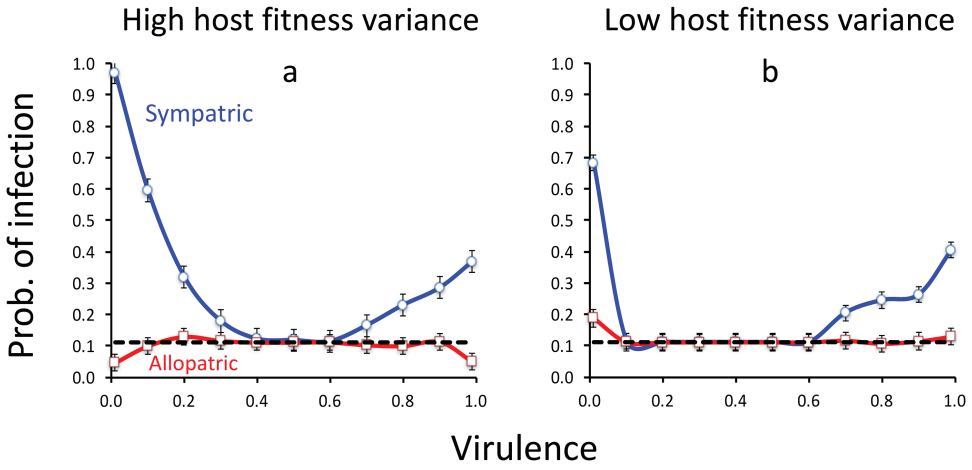

Figure 3. Variation in parasite fecundity. The parameters for panels **a** and **b** are identical to those in Figure 1a and 1b, respectively, except that the among-population variance in parasite fecundity, *B*, was reduced from 15 to 0.01. As in the previous figures, the difference between sympatric parasites (blue line) and allopatric parasites (red line) gives the degree of LA by parasites. Abbreviations and error bars are as given in Figure 1.

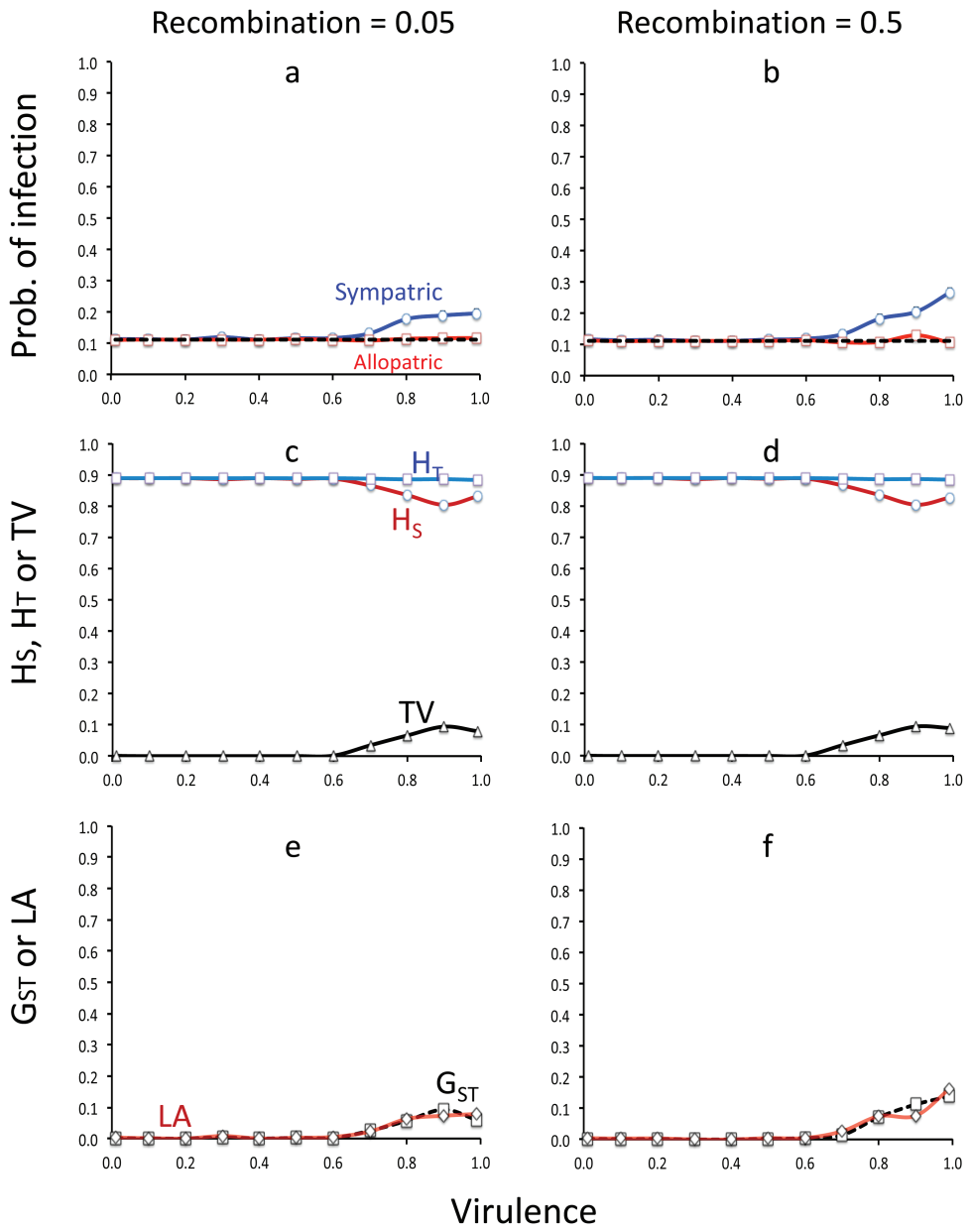

Figure 4. The effect of recombination in hosts on local adatation by parasites. The left-hand column gives the results for simulations where host recombination as low (rec = 0.05); the right-hand column gives the results were host was high (rec =0.5). The other parameters are the same as in Figure 1, except that the within-population standard deviation in host fecundity was reduced to 0.01. As in the previous figures, the difference between sympatric parasites (blue line) and allopatric parasites (red line) gives the degree of LA by parasites. Abbreviations and error bars are as given in Figure 1.

most common host genotypes in sympatric populations, producing a positive covariance between matching host and parasite genotypes. In contrast, the covariance between matching genotypes among allopatric combinations of host/parasite populations was effectively zero, and infection success was, on average, very near the random expectation of $1/H$, where H is the number of host genotypes. As a result of the positive covariance (on average) in sympatric host–parasite combinations, parasites were locally adapted. In addition, the measure of LA used here was very nearly equal to the standard measure of host population structure (G_{ST}). On the whole, under low virulence, it seems that spatial variation in fecundity selection produced host population structure, and that the parasites evolved to reflect this structure rather accurately.

A different set of results were observed under intermediate levels of virulence. Both host population-genetic structure (G_{ST}) and LA declined to near zero. However, it was not the case that LA declined because parasites became more successful at infecting allopatric hosts; the success of parasites on allopatric hosts remained at $1/H$. Rather, LA declined, because moderate parasite-mediated selection led to a decreased variance in the frequencies of host genotypes (thus increasing H_s). As the variance in host genotype frequencies was eroded, the covariance between matching host-parasite types was reduced to near zero, thereby eliminating LA (Supplementary Figure S1). In other words, the variance in h_i, which is required for a $\mathrm{cov}(p_i,h_i) > 0$, was eroded as parasite-mediated selection became stronger than fecundity selection. Similarly, G_{ST} declined as virulence

increased from low to moderate for the same reason. Frequency-dependent selection increased the average within-population genetic variance in the host, while having only a small effect on total variation in the metapopulation.

LA was again observed in the simulations at high levels of parasite virulence. This is consistent with previous results that show that strong parasite-mediated selection can destabilize the system leading to oscillatory dynamics in the frequencies of both host and parasite genotypes (Frank 1991; Ladle et al. 1993; Judson 1995; Gandon et al. 1996; Morand et al. 1996; Lively 1999; Gandon 2002; Sasaki et al. 2002; Gandon and Otto 2007). In the present study, the oscillations in host genotype frequencies are reflected in the average standard deviations for the frequencies of individual host genotypes over time (see TV in Figures 1c,d and 4c,d). Increases in these standard deviations are tightly coupled with decreases in H_s, and consequently with increases in G_{ST} at higher levels of virulence. Hence, Red Queen dynamics within populations results in host population structure. Here again, the degree of LA was almost identical to the measure for population structure (Figures 1e,f and 4e,f). While it is not surprising the LA and G_{ST} are correlated, it is perhaps surprising that they were almost exactly matched.

The basic results were robust to changing the relative migration rates of infected and uninfected hosts (Figure 2). However, the migration rates were low for all combinations of values. Increasing migration to higher levels would be expected to eventually swamp out local parasite adaptation (Lively 1999; Morgan et al. 2005; Gandon and Nuismer 2009). The results were also reasonably robust to reducing the variance in parasite fecundity among populations from 15 to 0.01 (compare Figures 1 and 3). Such a change should have reduced the variance in the strength of parasite-mediated selection among populations, but it did not greatly affect the patterns of local adaption across the virulence continuum.

Recombination breaks down the association between resistance genes in the host and host genes for fecundity. Hence, alleles that confer low fecundity in local populations are eliminated. Thus, parasite-mediated selection, even at low virulence, maintains high within-population variance in host genotype frequencies, and low among-population variance (Figure 4), as observed for MHC variation in natural populations of freshwater fish (Tobler et al. 2014). Hence, LA is not expected to be observed under low-to-moderate levels of virulence. It is only under high virulence that parasite-mediated selection against common host genotypes in strong enough to destabilize the system, leading to the oscillatory dynamics discussed above. This then gives rise to relatively weak, but detectable, LA (Figure 4). The reduced level of LA is likely due to the fact that recombination damps the oscillatory dynamics in outcrossing populations, which reduces host population structure (Figure 4). In general, parasite-mediated, negative frequency-dependent selection is more likely to be a homogenizing force in host metapopulations, rather than a diversifying force (Yoder and Nuismer 2010).

Taken together, the results suggest that LA by parasites should be most easily detected in clonal host populations occupying heterogeneous environments, especially when parasite virulence is very low or very high. Strong parasite LA has, in fact, been repeatedly observed in mixed clonal and sexual populations of freshwater snails that are coevolving with sterilizing digenetic trematodes (Lively 1989; Lively et al. 2004; King et al. 2009; King et al. 2011). Intermediate levels of parasite virulence can lead to the homogenization of host populations, which reduces the within-population covariance between matching host–parasite genotypes, and it reduces or eliminates LA. Finally, results also suggest that LA might be difficult to detect in sexual host populations. Hence, the variation in results uncovered in synthetic reviews (e.g., Greischar and Koskella 2007) should, perhaps, not be regarded as unexpected. Finally, the lack of local adaption in cross-inoculation experiments does not necessarily rule out coevolution. The lack of LA might actually be the direct result of coevolution.

Supplementary Material

Supplementary data are available at *Journal of Heredity* online.

Acknowledgments

I thank Lynda Delph for the invitation to participate in this symposium and for comments on the manuscript. I also thank Sylvain Gandon and 2 anonymous reviewers for helpful comments on a previous version of this article, and my lab group at Indiana University for helpful comments on oral presentations of the results.

Data Availability

In accordance with the *Journal of Heredity* data archiving policy (Baker 2013), the simulation model has been deposited in Dryad (doi:10.5061/dryad.r726b).

References

Agrawal AF, Lively CM. 2002. Infection genetics: gene-for-gene versus matching-allele models, and all points in between. *Evol Ecol Res*. 4:79–90.

Baker CS. 2013. Journal of heredity adopts joint data archiving policy. *J Hered*. 104:1.

Blanquart F, Kaltz O, Nuismer SL, Gandon S. 2013. A practical guide to measuring local adaptation. *Ecol Lett*. 16:1195–1205.

Bradshaw AD. 1960. Populations differentiation in *Agrostis tenuis* sibth. III. populations in varied environments. *New Phytol*. 59:92–103.

Clausen J, Keck DD, Hiesey WM. 1940. *Experimental studies on the nature of species. I: effect of varied environments on Western North American plants*. Washington (DC): Carnegie Institution of Washington. Publication 520.

Clausen J, Keck DD, Hiesey WM. 1948. *Experimental studies on the nature of species. III: environmental responses of climatic races of Achillea*. Washington (DC): Carnegie Institution of Washington. Publication 581.

Ebert D. 1994. Virulence and local adaptation of a horizontally transmitted parasite. *Science*. 265:1084–1086.

Engelstädter J. 2015. Host–parasite coevolutionary dynamics with generalized success/failure infection genetics. *Am Nat*. 185:E117–E129.

Engelstädter J, Bonhoeffer S. 2009. Red Queen dynamics with non-standard fitness interactions. *PLoS Comput Biol*. 5:e1000469.

Frank SA. 1991. Spatial variation in coevolutionary dynamics. *Evol Ecol*. 5:193–217.

Frank SA. 1993. Specificity versus detectable polymorphism in host–parasite genetics. *Proc Biol Sci*. 254:191–197.

Frank SA. 1994. Recognition and polymorphism in host–parasite genetics. *Philos Trans R Soc Lond B Biol Sci*. 346:283–293.

Gandon S. 2002. Local adaptation and the geometry of host–parasite coevolution. *Ecol Lett*. 5:246–256.

Gandon S, Capowiez Y, Dubois Y, Michalakis Y, Olivieri I. 1996. Local adaptation and gene-for-gene coevolution in a metapopulation model. *Proc R Soc Lond [Biol]*. 263:1003–1009.

Gandon S, Michalakis Y. 2002. Local adaptation, evolutionary potential and host–parasite coevolution: interactions between migration, mutation, population size and generation time. *J Evol Biol*. 15:451–462.

Gandon S, Nuismer SL. 2009. Interactions between genetic drift, gene flow, and selection mosaics drive parasite local adaptation. *Am Nat*. 173:212–224.

Gandon S, Otto SP. 2007. The evolution of sex and recombination in response to abiotic or coevolutionary fluctuations in epistasis. *Genetics*. 175:1835–1853.

Greischar MA, Koskella B. 2007. A synthesis of experimental work on parasite local adaptation. *Ecol Lett*. 10:418–434.

Hamilton WD. 1993. Haploid dynamic polymorphism in a host with matching parasites: effects of mutation/subdivision, linkage, and patterns of selection. *J Hered*. 84:328–338.

Hedrick PW. 2000. *Genetics of populations*. Sudberry (MA): Jones and Bartlett.

Hoeksema JD, Forde SE. 2008. A meta-analysis of factors affecting local adaptation between interacting species. *Am Nat*. 171:275–290.

Judson OP. 1995. Preserving genes: a model of the maintenance of genetic variation in a metapopulation under frequency-dependent selection. *Genet Res (Camb.)*. 65:175–191.

Kaltz O, Shykoff JA. 1998. Local adaptation in host–parasite systems. *Heredity*. 81:361–370.

Kawecki TJ, Ebert D. 2004. Conceptual issues in local adaptation. *Ecol Lett*. 7:1225–1241.

King KC, Delph LF, Jokela J, Lively CM. 2009. The geographic mosaic of sex and the Red Queen. *Curr Biol*. 19:1438–1441.

King KC, Delph LF, Jokela J, Lively CM. 2011. Coevolutionary hotspots and coldspots for host sex and parasite local adaptation in a snail–trematode interaction. *Oikos*. 120:1335–1340.

Koskella B. 2014. Bacteria–phage interactions across time and space: merging local adaptation and time shift experiments to understand phage evolution. *Am Nat*. 184:S9–S21.

Ladle RJ, Johnstone RA, Judson OP. 1993. Coevolutionary dynamics of sex in a metapopulation: escaping the Red Queen. *Proc R Soc Lond [Biol]*. 253:155–160.

Langerhans RB, Gifford ME, Joseph EO. 2007. Ecological speciation in Gambusia fishes. *Evolution*. 61:2056–2074.

Lascoux M, Glémin S, Savolainen O. 2016. *Local adaptation in plants*. In: eLS. Chichester: John Wiley& Sons, Ltd. p. 1–7; doi:10.1002/9780470015902.a0025270.

Lively CM. 1989. Adaptation by a parasitic trematode to local populations of its snail host. *Evolution*. 43:1663–1671.

Lively CM. 1999. Migration, virulence, and the geographic mosaic of adaptation by parasites. *Am Nat*. 153:S34–S47.

Lively CM. 2010. An epidemiological model of host–parasite coevolution and sex. *J Evol Biol*. 23:1490–1497.

Lively CM. 2016. Coevolutionary epidemiology: disease spread, local adaptation, and sex. *Am Nat*. 187:E77–E82.

Lively CM, Dybdahl MF, Jokela J, Osnas EE, Delph LF. 2004. Host sex and local adaptation by parasites in a snail–trematode interaction. *Am Nat*. 164(Suppl 5):S6–S18.

Maynard Smith J, Slatkin M. 1973. Stability of predator–prey systems. *Ecology*. 54:384–391.

Morand S, Manning SD, Woolhouse ME. 1996. Parasite–host coevolution and geographic patterns of parasite infectivity and host susceptibility. *Proc Biol Sci*. 263:119–128.

Morgan AD, Gandon S, Buckling A. 2005. The effect of migration on local adaptation in a coevolving host–parasite system. *Nature*. 437:253–256.

Morran LT, Parrish RC II, Gelarden IA, Allen MB, Lively CM. 2014. Experimental coevolution: rapid local adaptation by parasites depends on host mating system. *Am Nat*. 184(Suppl 1):S91–S100.

Nei M. 1973. Analysis of gene diversity in subdivided populations. *Proc Natl Acad Sci USA*. 70:3321–3323.

Nei M. 1977. *F*-statistics and analysis of gene diversity in subdivided populations. *Ann Hum Genet*. 41:225–233.

Nuismer SL. 2006. Parasite local adaptation in a geographic mosaic. *Evolution*. 60:24–30.

Nuismer SL. 2017. *Introduction to coevolutionary theory*. New York: W. H. Freeman.

Nuismer SL, Gandon S. 2008. Moving beyond common-garden and transplant designs: insight into the causes of local adaptation in species interactions. *Am Nat*. 171:658–668.

Otto SP, Michalakis Y. 1998. The evolution of recombination in changing environments. *Trends Ecol Evol*. 13:145–151.

Parker MA. 1985. Local population differentiation for compatibility in an annual legume and its host-specific fungal pathogen. *Evolution*. 39:713–723.

Richmond JQ, Reeder TW. 2002. Evidence for parallel ecological speciation in scincid lizards of the *Eumeces skiltonianus* species group (Squamata: Scincidae). *Evolution*. 56:1498–1513.

Sasaki A, Hamilton WD, Ubeda F. 2002. Clone mixtures and a pacemaker: new facets of Red-Queen theory and ecology. *Proc Biol Sci*. 269:761–772.

Savolainen O, Lascoux M, Merilä J. 2013. Ecological genomics of local adaptation. *Nat Rev Genet*. 14:807–820.

Schluter D. 1996. Ecological causes of adaptive radiation. *Am Nat*. 148:S40–S64.

Tobler M, Plath M, Riesch R, Schlupp I, Grasse A, Munimanda GK, Setzer C, Penn DJ, Moodley Y. 2014. Selection from parasites favours immunogenetic diversity but not divergence among locally adapted host populations. *J Evol Biol*. 27:960–974.

Turesson G. 1922. The genotypical response of plant species to the habitat. *Hereditas*. 3:211–350.

Williams GC. 1966. *Adaptation and natural selection*. Princeton: Princeton University Press.

Yoder JB, Nuismer SL. 2010. When does coevolution promote diversification? *Am Nat*. 176:802–817.

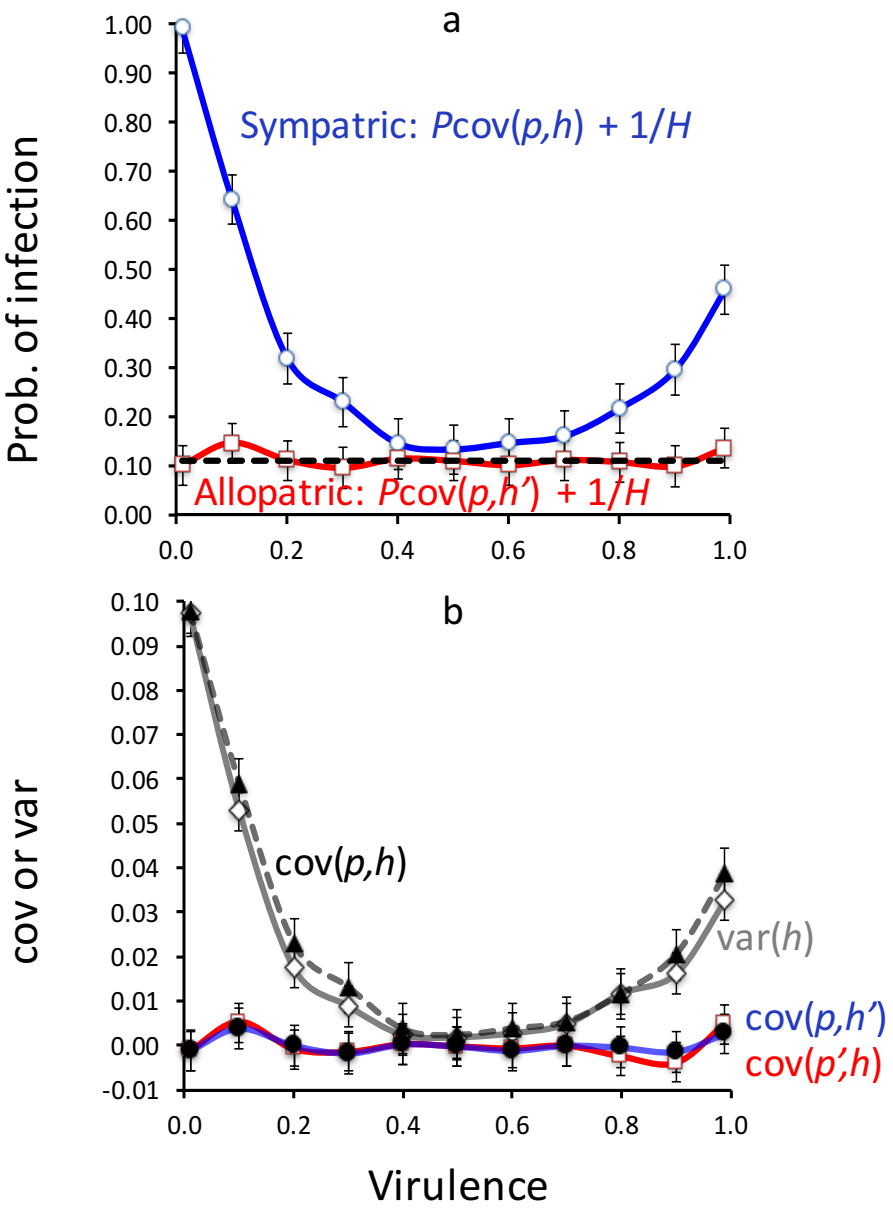

Supplemental Figure 1. Simulation results. a) The mean probability of infection for 20 sympatric (blue line) and 20 allopatric (red line) parasite populations. The dashed horizontal line gives the expected probability of infection if the covariance term is zero (=1/*H*). b) The mean covariance between matching host and parasite genotypes, cov(*p*,*h*) (dash line with filled triangles), the average variance in host genotype frequencies, var(*h*) (gray line with open diamonds), the mean covariance between parasite genotype frequencies and the matching host genotype frequencies in an allopatric host population, cov(*p*,*h*') (blue line with closed circles), and the mean covariance between host genotype frequencies and the matching parasite genotype frequencies in an allopatric parasite population, cov(*p*',*h*) (red line with open squares). Error bars give the 95% confidence interval of the mean (calculated as the average across all levels of virulence). All parameter values for these simulations are as reported in Fig. 1 in the main body of the text.

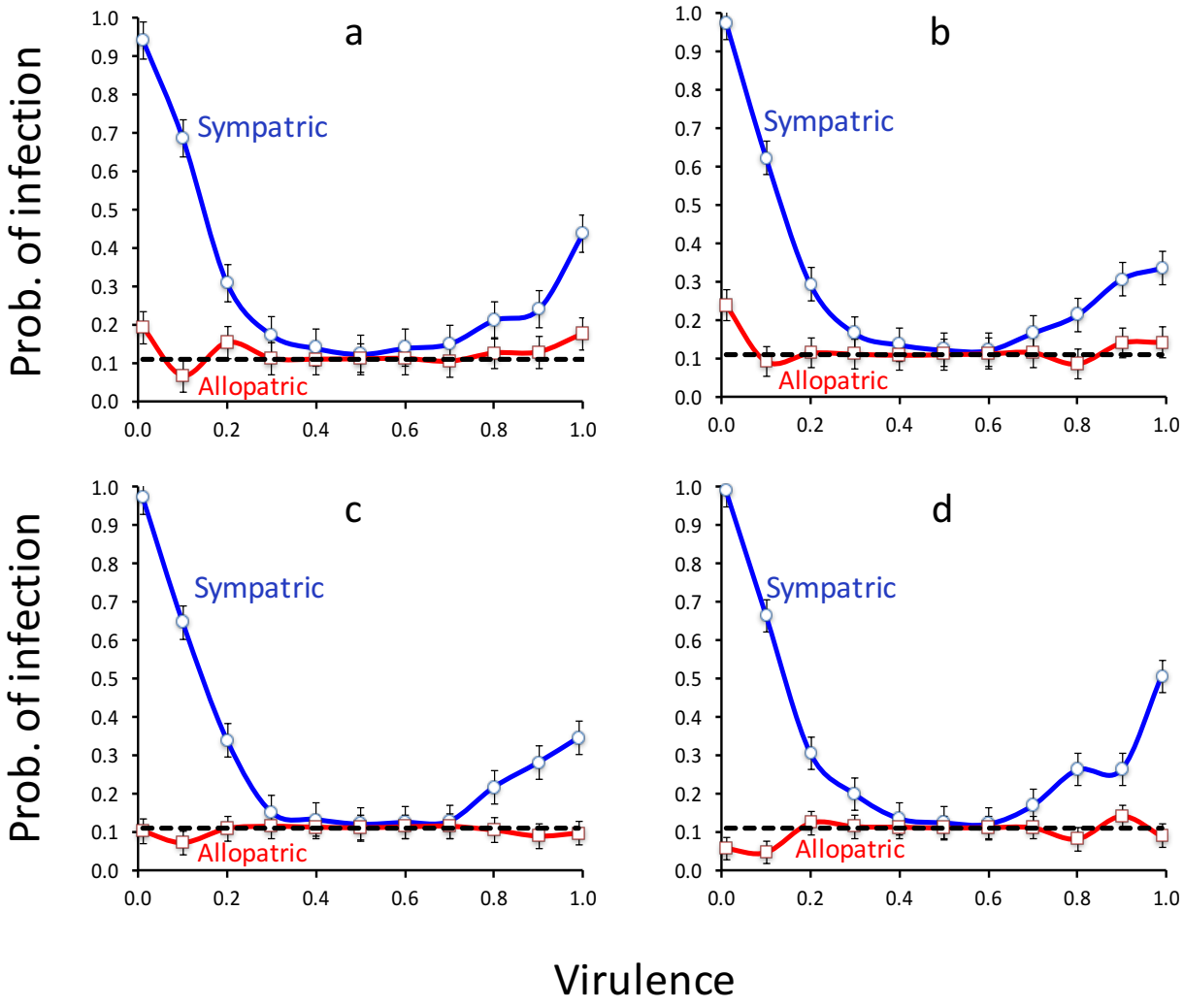

Supplemental Figure 2. Four replicate runs for the parameter values describe in Fig 1a. For all panels (a-d), the blue line (open circles) gives the average probability of infection per parasite propagule for hosts exposed to sympatric parasites (for 20 populations). The red line (open squares) gives the average probability of infection per parasite propagule for hosts exposed to allopatric parasites (for 20 populations). The dashed line gives the analytical prediction for infection when the covariance term for allopatric exposures is equal to zero.